

Modern Physics Letters B
 © World Scientific Publishing Company

The antiferromagnetic Potts model

Yacine Ikhlef

*Section Mathématiques, Université de Genève,
 2-4 rue du Lièvre, 1211 Genève, Switzerland
 yacine.ikhlef@unige.ch*

Received (Day Month Year)
 Revised (Day Month Year)

We review the exact results on the various critical regimes of the antiferromagnetic Q -state Potts model. We focus on the Bethe Ansatz approach for generic Q , and describe in each case the effective degrees of freedom appearing in the continuum limit.

Keywords: Potts model; Bethe Ansatz; Conformal Field Theory

1. Introduction

The Q -state Potts model¹, defined in 1952, is a lattice model for classical magnetism. Since the 1970's, it has been used as a laboratory to develop theoretical methods of Statistical Mechanics, such as Kramers-Wannier duality, Yang-Baxter integrability, Bethe Ansatz², Coulomb-gas formalism^{3,4}, Conformal Field Theory⁵ (CFT). Most studies on the Potts model deal with the *ferromagnetic* critical point, described by a Coulomb-Gas CFT or minimal CFT at the rational values. In contrast, the present review is concerned with the *antiferromagnetic* (AF) regime of the Potts model, which also contains exactly solvable critical points. Although it is based on the same simple lattice model, this regime exhibits interesting physical features. Indeed, non-unitarity of the equivalent vertex model allows a CFT with central charge $c > 1$, and non-compact degrees of freedom.

Let us introduce the subject with a short historical notice. In 1982, Baxter first discovered⁶ the location of the AF/paramagnetic transition by a mapping to a staggered integrable six-vertex (6V) model, and calculated the free energy density. Later on, Saleur described⁷ the complete phase diagram for $0 \leq Q \leq 4$, emphasizing the role of the Beraha numbers $Q = 4 \cos^2 \frac{\pi}{t}$ for integer t . At these values, he gave⁸ the CFT description of the AF/paramagnetic transition, relating it to the \mathbb{Z}_k parafermion CFT⁹. This transition corresponds to a staggered integrable model, but it appeared¹⁰ as a solution of the basic Yang-Baxter Equations (YBE) for the (N_α, N_β) Potts model. A complete CFT description of this transition for both generic and Beraha Q was achieved^{11,12}, especially through the study of the Bethe Ansatz equations: it consists in one compact boson ϕ_1 with Q -dependent radius

and one non-compact boson ϕ_2 . Besides the isotropic critical regimes mentioned so far, a mixed ferro-antiferromagnetic anisotropic regime was defined and solved¹³. Its continuum limit consists in two compact bosons: ϕ_1 with a Q -dependent radius, and ϕ_2 with a fixed radius, such that ϕ_2 decomposes into two Ising models.

This review is organised as follows. Section 2 is a reminder on the Potts model and its phase diagram for generic $0 \leq Q \leq 4$, and describes some related problems relevant to Statistical Mechanics, but also Condensed Matter Theory. There are three critical regimes for the Potts model with AF interactions. In Section 3, we summarize the methods used to study the critical points of the Potts model for generic values of Q . Sections 4, 5, 6 then apply these methods respectively to the BK phase, the AF transition line and the anisotropic critical regime. Section 7 concludes by mentioning some aspects that are not treated in detail by this review, together with some interesting open problems.

2. The Potts model and related Physics problems

2.1. Definitions and integrability properties

Let \mathcal{L} be a planar lattice. The Q -state Potts model on \mathcal{L} consists of spins S_j living on the vertices of \mathcal{L} , and taking the values $\{1, 2, \dots, Q\}$. The Boltzmann weight for a spin configuration is

$$W[\{S_j\}] = \exp \left(J \sum_{\langle i, j \rangle} \delta_{S_i, S_j} \right), \quad (1)$$

where δ stands for the Kronecker symbol and the product is on all edges of \mathcal{L} . A positive (resp. negative) value of J favors configurations where neighboring sites have equal (resp. distinct) spins. This defines the ferromagnetic and AF regimes.

The graphical expansion of the partition sum gives the Fortuin-Kasteleyn (FK) cluster model¹⁴ (see Fig 1):

$$Z_{\text{Potts}} = \sum_{G \subseteq \mathcal{L}} Q^{C(G)} v^{\ell(G)} := Z_{\text{FK}}(\mathcal{L}, Q, v), \quad v := e^J - 1, \quad (2)$$

where $C(G)$ is the number of connected components (clusters) of the subgraph G , and $\ell(G)$ is the number of edges in G . In this representation, Q plays the role of a real parameter, and we are mainly concerned with the regime $0 \leq Q \leq 4$. Using Euler's relation, the partition sum can be expressed as

$$Z_{\text{FK}}(\mathcal{L}, Q, v) = \text{const} \times \sum_{G' \subseteq \mathcal{L}'} Q^{C(G')} \left(\frac{Q}{v} \right)^{\ell(G')} = \text{const} \times Z_{\text{FK}}(\mathcal{L}', Q, Q/v), \quad (3)$$

where \mathcal{L}' is the lattice dual to \mathcal{L} . We refer to the transformation (3) as Kramers-Wannier duality.

The FK model can be, in turn, mapped to a loop model based on the Temperley-Lieb (TL) algebra¹⁵ (see Fig 1). The TL loop model lives on the medial lattice \mathcal{M}

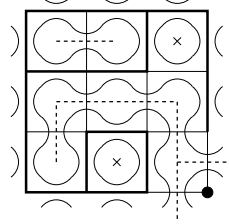


Fig. 1. Example FK cluster configuration on the square lattice \mathcal{L} , and corresponding loop configuration. Direct (resp. dual) clusters are shown as thick full (resp. dotted) lines, and clusters consisting of a single site as dots (resp. crosses).

consisting of the midpoints of the original lattice \mathcal{L} . A cluster configuration defines uniquely a loop configuration, by asking loops to separate direct and dual clusters. We have the relation

$$\text{const} \times Z_{\text{FK}}(\mathcal{L}, Q, v) = \sum_{\text{loop config. } H} n^{c(H)} x^{X(H)} := Z_{\text{loop}}, \quad \begin{cases} n = \sqrt{Q} \\ x = v/\sqrt{Q} \end{cases}, \quad (4)$$

where $c(H)$ is the number of closed loops in H , and $X(H)$ is the number of medial sites where the loops do not cross the original edge of \mathcal{L} . Although the Potts model can be defined on any planar lattice, we restrict the subsequent discussion to the square lattice for simplicity.

Consider the Potts model on a strip on width L sites (with L even), with coupling constant J_1 for horizontal edges, J_2 for vertical edges, and corresponding weights x_1, x_2 in the loop model. The transfer matrix for loops can be built with the TL algebra $\text{TL}_L(n)$. This algebra is generated by the operators e_j for $j = 1, \dots, L-1$, satisfying:

$$\begin{aligned} e_j^2 &= n e_j \\ e_j e_{j \pm 1} e_j &= e_j \\ e_j e_k &= e_k e_j \quad \text{for } |j - k| > 1. \end{aligned} \quad (5)$$

The transfer matrix parallel to one axis of the original lattice \mathcal{L} then reads

$$T_{\parallel} = \left[\prod_{j \text{ even}} (\mathbf{1} + x_1 e_j) \right] \left[\prod_{j \text{ odd}} (x_2 \mathbf{1} + e_j) \right]. \quad (6)$$

Our regime of interest is $0 \leq n \leq 2$. We introduce the *crossing parameter* γ and the parameter t , defined by

$$n = \sqrt{Q} = 2 \cos \gamma, \quad 0 \leq \gamma \leq \frac{\pi}{2}, \quad t := \frac{\pi}{\gamma}. \quad (7)$$

The algebra $\text{TL}_L(n)$ provides a solution to the YBE, with one spectral parameter u :

$$\check{R}_{j,j+1}(u) = \sin(\gamma - u) \mathbf{1} + \sin(u) e_j. \quad (8)$$

Table 1. The critical regimes of the Potts model on the square lattice. The last column gives the generic value of the central charge for the loop model.

self-dual	$0 < u < \gamma$	$x_1, x_2 > 0$	ferromagnetic critical	$c = 1 - \frac{6}{t(t-1)}$
	$\gamma < u < \pi/2$	$x_1, x_2 < 0$	BK phase	$c = 1 - \frac{6(t-1)^2}{t}$
staggered	$\gamma < u < \pi/2$	$x_1, x_2 < 0$	AF critical	$c = 2 - \frac{6}{t}$
	$0 < u < \gamma$	$x_1 > 0, x_2 < 0$	anisotropic critical	$c = 2 - \frac{12}{t(t-2)}$

2.2. Phase diagram

Let us recall the location^{2,6} of the critical points of the square-lattice Potts model.

- From (6) and (8), we see that the self-dual line $x_1 x_2 = 1$ corresponds to a homogeneous loop model with

$$x_1 = \frac{\sin u}{\sin(\gamma - u)}, \quad x_2 = \frac{1}{x_1}. \quad (9)$$

- The only other integrable case respecting the parity of sites in (6) is when spectral parameters alternate between u and $u + \frac{\pi}{2}$ ^{6,12,13}:

$$x_1 = \frac{\sin u}{\sin(\gamma - u)}, \quad x_2 = -\frac{\cos(\gamma - u)}{\cos u}. \quad (10)$$

Each of these two cases contains two critical regimes, corresponding to different values of the spectral parameters: see Table 1. The three isotropic critical regimes are shown in Fig. 2.

2.3. Related problems of Statistical Mechanics and Condensed Matter Theory

Using the FK formulation, one can relate the Potts model to various statistical models through exact equivalences.

- **Percolation.** At $Q = 1$, the FK model reduces to bond percolation on the lattice \mathcal{L} .
- **Uniform spanning trees.** In the limit ($Q \rightarrow 0, v = \sqrt{Q}$), using Euler's relation,

$$Q^{-\frac{1}{2}(\mathcal{N}+1)} Z_{\text{FK}}(\mathcal{L}, Q, \sqrt{Q}) \xrightarrow{Q \rightarrow 0} \# \text{ spanning trees on } \mathcal{L}, \quad (11)$$

where \mathcal{N} is the total number of sites in \mathcal{L} . So the continuum limit of the uniform spanning tree problem¹⁶ is determined by the ferromagnetic Potts transition at $Q \rightarrow 0$.

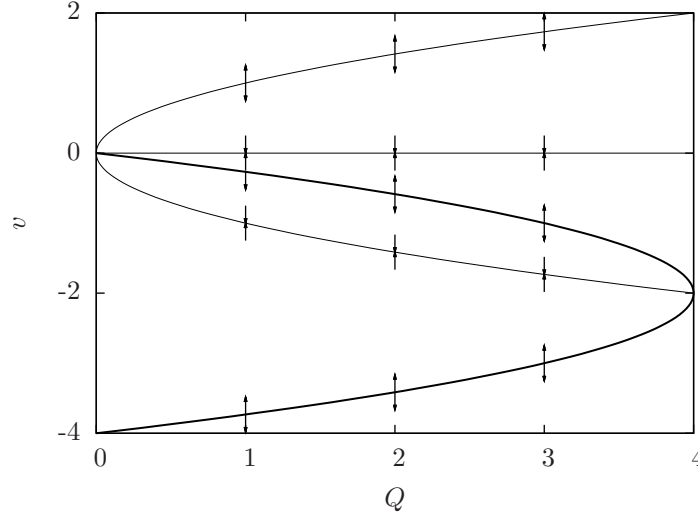


Fig. 2. Phase diagram of the isotropic Potts model on the square lattice. The self-dual line $v = \pm\sqrt{Q}$ is shown as a thin line, and the AF critical line $v = -2 \pm \sqrt{4-Q}$ as a thick line. The BK critical phase, governed by the self-dual branch $v = -\sqrt{Q}$, is enclosed in the thick line. Arrows represent the renormalization-group flows in the vicinity of fixed points.

- **Spanning forests.** In the vicinity of $Q = 0$, one can define another limit: $(Q \rightarrow 0, v = Q/w)$, where w is constant. Using the same arguments as above, we get the limit:

$$(Q/w)^{-(N+1)} Z_{\text{FK}}(\mathcal{L}, Q, Q/w) \xrightarrow{Q \rightarrow 0} \sum_{G \in \mathcal{F}(\mathcal{L})} w^{C(G)}, \quad (12)$$

where $\mathcal{F}(\mathcal{L})$ is the set of spanning forests¹⁷ on \mathcal{L} , *i.e.* spanning subgraphs with no internal face. The parameter w thus plays the role of a tree fugacity in the spanning forest problem. The phase diagram of the Potts model predicts¹⁸ the behavior of spanning forest as a function of w : if $w > 0$ or $w < -4$, the model is not critical (paramagnetic phase); if $-4 < w < 0$, the model is described by a Coulomb-Gas theory (BK phase); exactly at $w = -4$, the model is described by an $\text{OSP}(2|2)$ supersphere σ -model¹⁸.

- **Restricted Solid-On-Solid (RSOS) models.** At the Beraha numbers $\sqrt{Q} = 2 \cos \frac{\pi}{t}$ with integer $t \geq 4$, the TL generators can be represented as local operators in the A_{t-1} RSOS height model^{24,25}. The latter consists of local variables $\{h_j, j = 1, \dots, L\}$ subject to the local constraints

$$h_j \in \{1, \dots, t-1\}, \quad |h_j - h_{j+1}| = 1. \quad (13)$$

6 *Yacine Ikhlef*

The operators e_j are defined as

$$e_j |h_1 \dots h_L\rangle = \delta_{h_{j-1}, h_{j+1}} \sum_{h'=h_{j+1} \pm 1} \frac{\sqrt{\sin \frac{\pi h_j}{t} \sin \frac{\pi h'}{t}}}{\sin \frac{\pi h_{j+1}}{t}} |h_1 \dots h' \dots h_L\rangle. \quad (14)$$

The RSOS model may describe the statistics of a two-dimensional interface in three-dimensional space.

A second approach is to take the very anisotropic limit $u \rightarrow 0$, where the transfer matrix^a generates a local one-dimensional quantum Hamiltonian based on the $TL_L(n)$ algebra^b, and consider the spin- $\frac{1}{2}$ representation. The self-dual (9) and staggered (10) transfer matrices respectively give the Hamiltonians^{2,12}:

$$H_{\text{sd}} = \pm \sum_{j=1}^L e_j, \quad (15)$$

$$H_{\text{stag}} = \pm \sum_{j=1}^L (-n e_j + e_j e_{j+1} + e_{j+1} e_j). \quad (16)$$

The global minus sign in H_{sd} (resp. H_{stag}) corresponds to the ferromagnetic (resp. AF) critical point; the plus sign to the BK phase (resp. the anisotropic critical point).

The TL generators can be represented as rescaled projectors in the $U_q(\text{Sl}_2)$ quantum algebra¹⁹, where $q = e^{i\gamma}$. Consider a collection of L spin- $\frac{1}{2}$ variables $\{\sigma_j\}$. In terms of the Pauli matrices $\sigma_j^{x,y,z}$, the self-dual Hamiltonian describes an XXZ quantum spin chain²:

$$H_{\text{sd}} = \pm \frac{1}{2} \sum_{j=1}^L (\sigma_j^x \sigma_{j+1}^x + \sigma_j^y \sigma_{j+1}^y - \cos \gamma \sigma_j^z \sigma_{j+1}^z) + \text{const}. \quad (17)$$

If we denote $P_{j,j+1}^{(0)}$ the projector of $(\sigma_j + \sigma_{j+1})$ onto total spin zero, then the operators $e_j := n P_{j,j+1}^{(0)}$ satisfy the $TL_L(n)$ relations (5). Furthermore, the projector of $(\sigma_j + \sigma_{j+1} + \sigma_{j+2})$ onto total spin $\frac{3}{2}$ is given by

$$P_{j,j+1,j+2}^{(3/2)} = 1 + \frac{(e_j e_{j+1} + e_{j+1} e_j) - n(e_j + e_{j+1})}{n^2 - 1}.$$

In terms of the $U_q(\text{Sl}_2)$ projectors, the staggered Hamiltonian reads²⁰

$$H_{\text{stag}} = \pm \sum_{j=1}^L \left[n^2 P_{j,j+1}^{(0)} + (n^2 - 1) P_{j,j+1,j+2}^{(3/2)} \right]. \quad (19)$$

If the plus sign is chosen and $n > 1$, the second term in (19) favors a totally dimerized state (a product of $L/2$ $U_q(\text{Sl}_2)$ singlets), while the first term gives additional

^a We consider here the transfer matrix parallel to one axis of the medial lattice \mathcal{M} .

^b We use a periodic variant of $TL_L(n)$, with $e_{j \pm L} := e_j$.

energy to dimerized pairs of neighbours: the spin chain is thus subject to frustration. So H_{stag} is an integrable, q -deformed generalization of the well-studied $\text{SU}(2)$ frustrated spin chain^{21,22,23}.

3. General approach to the solution

3.1. Equivalent vertex model, twisted BC

We consider the Potts model on the lattice L , embedded in a cylinder. Its exact solution is obtained through the sequence of mappings²:

$$(\text{Potts on } \mathcal{L}) \longrightarrow (\text{FK on } \mathcal{L}) \longrightarrow (\text{TL on } \mathcal{M}) \longrightarrow (6V \text{ on } \mathcal{M}).$$

The resulting 6V model is homogeneous for self-dual Potts, and staggered for the AF and anisotropic critical lines. The last mapping is done by orienting independently each loop, and giving it a weight $e^{\pm i\gamma}$ according to its orientation, so that the total weight for a loop is $n = 2 \cos \gamma$. The complex weight $e^{\pm i\gamma}$ is distributed locally in the 6V model, by counting the local turns of each loop fragment². However, through this mapping, the loops which wind around the cylinder (*non-contractible loops*) receive an incorrect weight $\tilde{n} = 2$, because their total rotation angle is zero in both orientations. To correct this, we consider the 6V with a seam along the axis of the cylinder: an arrow which crosses the seam from left to right (resp. from right to left) gets a factor $e^{i\varphi}$ (resp. $e^{-i\varphi}$). Non-contractible loops then get a weight

$$\tilde{n} = 2 \cos \varphi. \quad (21)$$

The Potts ground state corresponds to $\varphi = \gamma$, but it can be useful to consider other values of φ , *e.g.*, to compute the magnetic exponent of the Potts model (see below).

3.2. Analysis of the BAE

The integrable 6V is solvable by Bethe Ansatz. In all the cases we consider here, the Bethe roots sit on horizontal line(s) in the complex plane, and are described by a root density ρ in the large- L limit. One may extract from the BAE two types of data which are relevant to the associated critical theory:

- The physical properties of elementary excitations (particle-hole excitations in the root distribution) are derived easily by Fourier transform. This leads to the scattering theory of these quasi-particles both at criticality and in the vicinity of the critical point.
- The finite-size corrections to the energies allow us to relate the lattice model to CFT, where the energies and momenta are expected to behave as

$$E_0 \simeq e_\infty L - \frac{\pi v c}{6L}, \quad (22)$$

$$E_{h,\bar{h}} \simeq E_0 + \frac{2\pi v}{L}(h + \bar{h}), \quad (23)$$

$$k_{h,\bar{h}} \equiv \frac{2\pi}{L}(h - \bar{h}) \mod 2\pi, \quad (24)$$

where E_0 is the ground-state energy, e_∞ is the energy density, v is the Fermi velocity, c is the central charge and $E_{h,\bar{h}}, k_{h,\bar{h}}$ are the energy and total momentum associated to the primary state with dimensions (h, \bar{h}) . The computation of the finite-size corrections involves the Wiener-Hopf technique, described in this context by Yang and Yang²⁶.

3.3. Numerical transfer-matrix computations

Analytical results may be checked numerically by computing the dominant eigenvalues of the transfer matrix in various sectors or, equivalently, the lowest eigenvalues of the Hamiltonian. Through (22)-(23), the eigenvalues provide numerical estimates for the central charge and conformal dimensions.

Using the TL formulation, one usually computes systems of up to $L = 20$ sites, and the precision obtained for the exponents is about 10^{-3} (except in the presence of logarithmic corrections, typically at $\gamma \rightarrow 0$).

4. The Berker-Kadanoff phase

4.1. Relation to the XXZ spin chain

The two branches of the self-dual line (9) are related to each other by $(x_1, x_2) \rightarrow (-x_1, -x_2)$, or equivalently by $\sqrt{Q} \rightarrow -\sqrt{Q}$ (see (5)). We denote $\mu := \pi - \gamma$, so that $-\sqrt{Q} = 2 \cos \mu$. In the very anisotropic limit $u \rightarrow 0$, the BK critical line is thus equivalent to an XXZ spin chain with twisted BC:

$$H_{\text{XXZ}} := -\frac{1}{2} \sum_{j=1}^L (\sigma_j^x \sigma_{j+1}^x + \sigma_j^y \sigma_{j+1}^y + \Delta \sigma_j^z \sigma_{j+1}^z), \quad \sigma_{L+1}^\pm := e^{\pm 2i\varphi} \sigma_1^\pm, \quad (25)$$

where

$$\Delta = -\cos \mu, \quad \varphi = \mu. \quad (26)$$

In the present Section, we will then recall Bethe-Ansatz results on XXZ, and their application to the study of the BK phase for generic Q .

On each site of the XXZ chain, we consider an up spin as an empty site, and a down spin as a particle. The Bethe Ansatz Equations and eigenvalues for r particles read:

$$\left[\frac{\sinh(\frac{i\mu}{2} - \lambda_j)}{\sinh(\frac{i\mu}{2} + \lambda_j)} \right]^L = (-1)^{r-1} e^{2i\varphi} \prod_{\ell=1}^r \frac{\sinh(i\mu - \lambda_j + \lambda_\ell)}{\sinh(i\mu + \lambda_j - \lambda_\ell)}, \quad (27)$$

$$E = \sum_{j=1}^r \epsilon(\lambda_j) = \sum_{j=1}^r \frac{-2 \sin^2 \mu}{\cosh \lambda_j - \cos \mu}. \quad (28)$$

4.2. The ground state and the quasi-particle picture

We take the logarithmic form of the BAE:

$$Lk(\lambda_j) = 2\pi I_j + 2\varphi - \sum_{\ell=1}^r \Theta(\lambda_j - \lambda_\ell), \quad (29)$$

where

$$k(\lambda) := -i \log \frac{\sinh(i\frac{\mu}{2} - \lambda)}{\sinh(i\frac{\mu}{2} + \lambda)}, \quad \Theta(\lambda) := -i \log \frac{\sinh(i\mu + \lambda)}{\sinh(i\mu - \lambda)}, \quad (30)$$

and the “Bethe integers” I_j are half-odd integers (resp. integers) if r is even (resp. odd). In the large- L limit, the Bethe roots λ_j are described by a root density $\rho(\lambda)$, satisfying the linear integral equation

$$k'(\lambda) = 2\pi\rho(\lambda) - \int_{\Lambda_-}^{\Lambda_+} d\nu \rho(\nu) K(\lambda - \nu), \quad (31)$$

where the kernel K is given by $K := \Theta'$, and Λ_\pm are the extremal values of the λ_j 's.

The ground state for $\varphi = 0$ corresponds to a symmetric root distribution with $r = L/2$ and $\Lambda_\pm = \pm\infty$, so (31) becomes solvable by Fourier transform. We use the notations

$$\widehat{f}(\omega) := \int_{-\infty}^{+\infty} d\lambda f(\lambda) e^{i\omega\lambda}, \quad (f \star g)(\lambda) := \int_{-\infty}^{+\infty} d\nu f(\nu) g(\lambda - \nu). \quad (32)$$

The ground-state solution is

$$\rho_0(\lambda) = \frac{1}{2\mu \cosh \frac{\pi\lambda}{\mu}}, \quad \widehat{\rho}_0(\omega) = \frac{1}{2 \cosh \frac{\mu\omega}{2}}. \quad (33)$$

Any physical quantity is given by an integral of the form

$$A(\rho) = \int_{\Lambda_-}^{\Lambda_+} d\lambda \rho(\lambda) a(\lambda), \quad (34)$$

where, *e.g.*, $a = 1$ for the particle density, $a = k$ for the total momentum, *etc.* A hole at position λ_h in the root distribution produces a variation in A , given by the dressed quantity²⁷ \widetilde{a} :

$$A(\rho) - A(\rho_0) = -\frac{1}{L} \left[\left(1 - \frac{K}{2\pi} \right)^{-1} \star a \right] (\lambda_h) := -\frac{1}{L} \widetilde{a}(\lambda_h). \quad (35)$$

In particular, the dispersion relation of the quasi-particles is given by:

$$\widetilde{k}(\lambda) = 2\text{Arctan} \left(\tanh \frac{\pi\lambda}{2\mu} \right), \quad \widetilde{\epsilon}(\lambda) = -\frac{\pi \sin \mu}{\mu \cosh \frac{\pi\lambda}{\mu}}. \quad (36)$$

Close to the Fermi levels $\widetilde{k}_F = \pm \frac{\pi}{2}$, this becomes a linear relation:

$$\widetilde{\epsilon} \simeq v |\widetilde{k} - \widetilde{k}_F|, \quad v = \frac{\pi \sin \mu}{\mu}. \quad (37)$$

10 *Yacine Ikhlef*

To complete the S -matrix picture, one defines the dressed scattering amplitudes as follows. Consider a root distribution with particles of density ρ and holes of density ρ_h . The BAE then read

$$k' = 2\pi(\rho + \rho_h) - K \star \rho. \quad (38)$$

Introducing $\Phi := (2\pi - K)^{-1} \star (-2\pi K)$, we express the BAE as

$$\tilde{k}' = 2\pi(\rho + \rho_h) - \Phi \star \rho_h. \quad (39)$$

In the above form, the BAE describe the scattering of holes with momentum \tilde{k} and scattering amplitude

$$S(\lambda, \lambda') = \exp \left[i \int_0^{\lambda - \lambda'} d\nu \Phi(\nu) \right] \quad (40)$$

$$= \exp \left[-i \int_{-\infty}^{+\infty} \frac{d\omega}{\omega} \frac{\sinh\left(\mu - \frac{\pi}{2}\right)\omega \sin(\lambda - \lambda')\omega}{2 \cosh \frac{\mu\omega}{\pi} \sinh \frac{\pi - \mu}{2}\omega} \right]. \quad (41)$$

4.3. CFT spectrum

In this paragraph, we use the BAE to derive the CFT associated to the *untwisted* ($\varphi = 0$) spin chain. In the next paragraph, we will then reintroduce the twist to compute correctly the critical exponents in the Potts model.

As explained above, the CFT spectrum is obtained through the finite-size corrections to the energies. The central charge is given by the ground-state energy E_0 . In this case, the corrections are easily computed²⁷ using the Euler-Maclaurin formula. This gives

$$E_0 \simeq L \int_{-\infty}^{+\infty} d\lambda \rho_0(\lambda) \epsilon(\lambda) - \frac{\pi v}{6L}, \quad (42)$$

and so the central charge is $c = 1$.

The states corresponding to primary operators in the CFT are combinations of “magnetic” and “electric” excitations. A magnetic excitation of charge $m \in \mathbb{Z}$ consists in removing m roots from the ground state, and arranging the Bethe integers I_j symmetrically around zero. An electric excitation of charge $e \in \mathbb{Z}$ is a global shift of all Bethe integers: $I_j \rightarrow I_j - e$. The associated energy corrections may be computed by the Wiener-Hopf technique²⁶. This results in the expression

$$E_{e,m} \simeq E_0 + \frac{2\pi v}{L} \left(\frac{gm^2}{2} + \frac{e^2}{2g} \right), \quad g = \frac{\pi - \mu}{\pi}. \quad (43)$$

On the other hand, the total momentum for the (e, m) excitation is

$$k_{e,m} = \frac{2\pi}{L} \sum_{j=1}^r I_j \equiv \frac{2\pi em}{L} \pmod{2\pi}. \quad (44)$$

From $E_{e,m}$ and $k_{e,m}$, we deduce the conformal dimensions:

$$h_{e,m} = \frac{1}{4} \left(\frac{e}{\sqrt{g}} + m\sqrt{g} \right)^2, \quad \bar{h}_{e,m} = \frac{1}{4} \left(\frac{e}{\sqrt{g}} - m\sqrt{g} \right)^2, \quad g = \frac{\pi - \mu}{\pi}. \quad (45)$$

We call $\mathcal{O}_{e,m}$ the corresponding primary operator in the CFT. One can also identify the Bethe root configurations associated to the descendants of $\mathcal{O}_{e,m}$: the action of the Virasoro generator L_{-n} (resp. \bar{L}_{-n}) amounts to shifting the highest (resp. lowest) Bethe integer by n (resp. $-n$).

The central charge $c = 1$, the primary dimensions (45) and the Virasoro descendants obtained by this analysis of the BAE correspond to a compactified boson (or Coulomb gas) CFT with action^{3,4}

$$\mathcal{A} = \frac{g}{4\pi} \int d^2x (\nabla\phi)^2, \quad \phi \equiv \phi + 2\pi. \quad (46)$$

In this theory, a magnetic excitation is a dislocation defect of amplitude $2\pi m$, whereas an electric excitation corresponds to the insertion of the vertex operator $\exp(i e \phi)$.

The continuum partition sum on a torus of modular ratio τ has the form:

$$Z_{6V} = \frac{1}{|\eta(q)|^2} \sum_{e,m \in \mathbb{Z}} q^{h_{em}} \bar{q}^{\bar{h}_{em}}, \quad q := e^{2i\pi\tau}, \quad (47)$$

where η is the Dedekind function.

4.4. Effective central charge and critical exponents

In the presence of a twist φ , the conformal dimensions (45) are modified by the change of electric charges

$$e \rightarrow e + \frac{\varphi}{\pi}. \quad (48)$$

The effective central charge and critical exponents for the Potts model in the BK phase are obtained by considering the appropriate sectors for m and φ in the 6V model.

The Potts ground state has charges ($e_0 = \mu/\pi, m = 0$), and hence the effective central charge for the Potts model is

$$c_{\text{eff}} = 1 - \frac{6(1-g)^2}{g} = 1 - \frac{6(t-1)^2}{t}. \quad (49)$$

The magnetic, ℓ -leg watermelon and thermal exponents X_H , X_ℓ and X_T are defined through the relations

$$G_H(r, r') := \left\langle \delta_{S_r, S_{r'}} - \frac{1}{Q} \right\rangle \simeq |r - r'|^{-2X_H}, \quad (50)$$

$$G_\ell(r, r') := \mathbb{P}[r, r' \text{ are connected by } \ell \text{ strands}] \simeq |r - r'|^{-2X_\ell}, \quad (51)$$

$$\xi \simeq |v - v_c|^{-\nu}, \quad X_T := 2 - \frac{1}{\nu}, \quad (52)$$

where ξ is the correlation length and $v_c = -\sqrt{Q}$ is the RG fixed point for the BK phase.

- The magnetic correlation function may be written as

$$G_H(r, r') = (1 - Q^{-1}) \frac{Z_H(r, r')}{Z}, \quad (53)$$

where $Z_H(r, r')$ is the partition sum of FK configurations where r and r' belong to the same cluster. In the cylinder geometry, we put r and r' at the ends of the cylinder, and the constraint for Z_H is equivalent to forbidding any non-contractible loop: this is easily implemented by setting $\varphi = \pi/2$, so that $\tilde{n} = 0$. Hence, the magnetic exponent is

$$X_H = \frac{(1/2)^2}{2g} - \frac{e_0^2}{2g} = \frac{1/4 - (1-g)^2}{2g}. \quad (54)$$

- The watermelon exponents correspond to higher magnetization sectors. Note that ℓ has to be even when L is even. Exponent X_ℓ corresponds to the charges $(e = 0, m = \ell/2)$, and hence:

$$X_\ell = \frac{g\ell^2}{8} - \frac{(1-g)^2}{2g}. \quad (55)$$

- The thermal exponent X_T corresponds to an irrelevant perturbation around $v = -\sqrt{Q}$ (see Fig. 2), and thus we expect $X_T \geq 2$. In the sector $m = 0$, non-contractible loops are allowed, and the twist must be of the form $\varphi = \pi(e_0 + p)$, with integer p . This leads to the series of exponents

$$X_T(p) = \frac{(e_0 + p)^2 - e_0^2}{2g}. \quad (56)$$

The two lowest exponents in this series correspond to the values $p = -2, 1$:

$$X_T = 2, \quad X'_T = \frac{3}{2g} - 1 \geq 2 \quad (57)$$

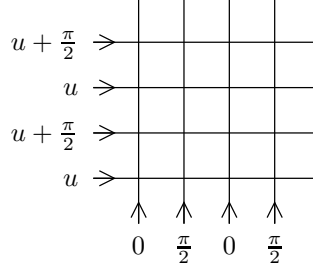
5. The antiferromagnetic critical line

5.1. The \mathbb{Z}_2 staggered vertex model

The antiferromagnetic critical line is mapped to the staggered 6V model with an alternation of spectral parameters, as shown in Fig. 3. We consider this model on a cylinder of circumference $L = 2N$ sites. Since it is built on the TL algebra, the transfer matrix has $U_q(\text{Sl}_2)$ invariance. Moreover, the YBE imply an additional symmetry, expressed by the “ \mathbb{Z}_2 conjugation operator” C :

$$C := \prod_{j=1}^N \left(-\frac{\check{R}(\frac{\pi}{2})}{\cos \gamma} \right). \quad (58)$$

The operator C satisfies $C^2 = \mathbf{1}$ and commutes with the transfer matrix. As a consequence, the eigenstates may be labelled according to this \mathbb{Z}_2 symmetry.

Fig. 3. Spectral parameters of the \mathbb{Z}_2 staggered vertex model.

5.2. Bethe Ansatz Equations

The BAE and energies for the \mathbb{Z}_2 staggered model read, for even N :

$$\left[\frac{\sinh(i\gamma + \alpha_j)}{\sinh(i\gamma - \alpha_j)} \right]^N = (-1)^{r-1} e^{2i\varphi} \prod_{\ell=1}^r \frac{\sinh \frac{1}{2}(2i\gamma + \alpha_j - \alpha_\ell)}{\sinh \frac{1}{2}(2i\gamma - \alpha_j + \alpha_\ell)}, \quad (59)$$

$$E = \sum_{j=1}^r \frac{2 \sin^2 2\gamma}{\cosh 2\alpha_j - \cos 2\gamma}. \quad (60)$$

The Bethe roots α_j are individually defined *modulo* $2i\pi$, but the BAE are invariant under a global shift $\alpha_j \rightarrow \alpha_j + i\pi$. This reflects the \mathbb{Z}_2 invariance discussed above, and in fact, one can prove¹² that the conjugation operator C acts as follows on the Bethe eigenstates $|\psi(\alpha_1, \dots, \alpha_r)\rangle$:

$$C|\psi(\alpha_1, \dots, \alpha_r)\rangle = \text{const} \times |\psi(\alpha_1 + i\pi, \dots, \alpha_r + i\pi)\rangle. \quad (61)$$

The expression (60) for the energy suggests that Bethe roots α_j lie on the lines $\text{Im } \alpha = \pm \frac{i\pi}{2}$, so that their contribution to the energy is negative. Hence, we divide the roots into two sets

$$\alpha_j^0 = \lambda_j^0 + \frac{i\pi}{2}, \quad \alpha_j^1 = \lambda_j^1 - \frac{i\pi}{2}. \quad (62)$$

We denote r^a the number of roots λ_j^a . In terms of the λ_j^a , the BAE and energies read

$$\exp [iNk(\lambda_j^a)] = (-1)^{r^a-1} e^{2i\varphi} \prod_{b=0,1} \prod_{\ell=1}^{r^b} \exp [-i\Theta^{a-b}(\lambda_j^a - \lambda_\ell^b)], \quad (63)$$

$$E = \sum_{a=0,1} \sum_{j=1}^{r^a} \epsilon(\lambda_j^a) = \sum_{a=0,1} \sum_{j=1}^{r^a} \frac{-2 \sin^2 2\gamma}{\cosh 2\lambda_j^a + \cos 2\gamma}, \quad (64)$$

where:

$$k(\lambda) := -i \log \frac{\cosh(i\gamma + \lambda)}{\cosh(i\gamma - \lambda)}, \quad (65)$$

$$\Theta^0(\lambda) := -i \log \frac{\sinh(i\gamma - \frac{\lambda}{2})}{\sinh(i\gamma + \frac{\lambda}{2})}, \quad \Theta^{\pm 1}(\lambda) := -i \log \frac{\cosh(i\gamma - \frac{\lambda}{2})}{\cosh(i\gamma + \frac{\lambda}{2})}. \quad (66)$$

In these notations, the \mathbb{Z}_2 conjugation (61) exchanges the indices $a = 0, 1$.

5.3. *XXZ states*

If we denote $\mu = \pi - 2\gamma$, then we have the identities

$$k(\lambda) = -i \log \frac{\sinh(\frac{i\mu}{2} - \lambda)}{\sinh(\frac{i\mu}{2} + \lambda)}, \quad (67)$$

$$(\Theta^0 + \Theta^{\pm 1})(\lambda) = -i \log \frac{\sinh(i\mu + \lambda)}{\sinh(i\mu - \lambda)}, \quad (68)$$

$$\epsilon(\lambda) = \frac{-2 \sin^2 \mu}{\cosh 2\lambda - \cos \mu}. \quad (69)$$

Hence, if the sets $\{\lambda_j^0\}$ and $\{\lambda_j^1\}$ are identical, the BAE and energies are equivalent to those of the XXZ spin chain with parameter μ and twist φ .

5.4. *Ground state and quasi-particles*

The discussion of Section 4 on the large- L limit of the BAE can be adapted to the \mathbb{Z}_2 staggered model, except we now have two coupled sets of BAE satisfying \mathbb{Z}_2 symmetry. The logarithmic form of the BAE is

$$Nk(\lambda_j^0) = 2\pi I_j^0 + 2\varphi - \sum_{\ell=1}^{r^0} \Theta^0(\lambda_j^0 - \lambda_\ell^0) - \sum_{\ell=1}^{r^1} \Theta^{-1}(\lambda_j^0 - \lambda_\ell^1), \quad (70)$$

$$Nk(\lambda_j^1) = 2\pi I_j^1 + 2\varphi - \sum_{\ell=1}^{r^0} \Theta^1(\lambda_j^1 - \lambda_\ell^0) - \sum_{\ell=1}^{r^1} \Theta^0(\lambda_j^1 - \lambda_\ell^1), \quad (71)$$

where the I_j^a are half-odd integers (resp. integers) if r^a is even (resp. odd). In the large- N limit, the roots lie on the intervals $[\Lambda_-^0, \Lambda_+^0]$ and $[\Lambda_-^1, \Lambda_+^1]$, and the BAE become

$$k'(\lambda) = 2\pi \rho^a(\lambda) - \sum_{b=0,1} \int_{\Lambda_-^b}^{\Lambda_+^b} d\nu \rho^b(\nu) K^{a-b}(\lambda - \nu), \quad (72)$$

where $K^a := (\Theta^a)'$. The ground state is a particular case of the XXZ states described in Section 5.3, and hence the ground-state root densities are

$$\rho^0(\lambda) = \rho^1(\lambda) = \rho_0(\lambda) = \frac{1}{2\mu \cosh \frac{\pi\lambda}{\mu}}. \quad (73)$$

A physical quantity reads

$$A(\rho^0, \rho^1) = \int_{\Lambda_-^0}^{\Lambda_+^0} d\lambda \rho^0(\lambda) a(\lambda) + \int_{\Lambda_-^1}^{\Lambda_+^1} d\lambda \rho^1(\lambda) a(\lambda) \quad (74)$$

We introduce the linear combinations $K^\pm := K^0 \pm K^1$. The presence of a hole λ_h^0 in the root distribution $\{\lambda_j^0\}$ results in the change:

$$A(\rho^0, \rho^1) - A(\rho_0, \rho_0) = -\frac{1}{N} \left[\left(1 - \frac{K^+}{2\pi} \right)^{-1} \star a \right] (\lambda_h^0) := \tilde{a}(\lambda_h^0). \quad (75)$$

So, from (67)–(69), the elementary excitations have the same dispersion relation (36) as in the XXZ chain. The important difference with XXZ is that there are now two kinds (0, 1) of quasi-particles, and their dressed scattering amplitudes depend on the type of quasi-particles. The BAE in the presence of holes read

$$\begin{cases} k' = 2\pi(\rho^0 + \rho_h^0) - K^0 \star \rho^0 - K^{-1} \star \rho^1 \\ k' = 2\pi(\rho^1 + \rho_h^1) - K^1 \star \rho^0 - K^0 \star \rho^1. \end{cases} \quad (76)$$

We put them in “diagonal form”:

$$\begin{cases} 2k' = 2\pi(\rho^+ + \rho_h^+) - K^+ \star \rho^+ \\ 0 = 2\pi(\rho^- + \rho_h^-) - K^- \star \rho^-. \end{cases} \quad (77)$$

where $\rho^\pm = \rho^0 \pm \rho^1$. We can then express the BAE in terms of the ρ_h^\pm :

$$\begin{cases} 2\tilde{k}' = 2\pi(\rho^+ + \rho_h^+) - \Phi^+ \star \rho_h^+ \\ 0 = 2\pi(\rho^- + \rho_h^-) - \Phi^- \star \rho_h^-. \end{cases} \quad (78)$$

where $\Phi^\pm := (2\pi - K^\pm)^{-1} \star (-2\pi K^\pm)$. Finally, we get the dressed BAE:

$$\tilde{k}' = 2\pi(\rho^a + \rho_h^a) - \sum_{b=0,1} \Phi^{a-b} \star \rho_h^b, \quad (79)$$

where $\Phi^0 := \frac{1}{2}(\Phi^+ + \Phi^-)$ and $\Phi^1 = \Phi^{-1} := \frac{1}{2}(\Phi^+ - \Phi^-)$. The scattering amplitude between particles of types a and b is then

$$S^{a,b}(\lambda, \lambda') = \exp \left[i \int_0^{\lambda-\lambda'} d\nu \Phi^{a-b}(\nu) \right]. \quad (80)$$

We give the kernels Φ^a in Fourier space:

$$\hat{\Phi}^0(\omega) = \frac{-2\pi \cosh(\pi - 3\gamma)\omega}{2 \sinh \gamma \omega \sinh(\pi - 2\gamma)\omega}, \quad \hat{\Phi}^{\pm 1}(\omega) = \frac{2\pi \cosh \gamma \omega}{2 \sinh \gamma \omega \sinh(\pi - 2\gamma)\omega}. \quad (81)$$

5.5. CFT spectrum

The CFT describing the staggered vertex model is a combination of two bosons ϕ_1 and ϕ_2 , with action (see (46))

$$\mathcal{A} = \frac{1}{4\pi} \int d^2x \left[g_1 (\nabla \phi_1)^2 + g_2 (\nabla \phi_2)^2 \right], \quad \phi_\alpha \equiv \phi_\alpha + 2\pi, \quad (82)$$

where

$$g_1 = \frac{\gamma}{\pi}, \quad g_2 \xrightarrow[N \rightarrow \infty]{} 0. \quad (83)$$

As it is done for the XXZ model in Section 4.3, the above action is inferred from the central charge and operator content of the BAE. Since the ground state is of the XXZ type and the Fermi velocity has the XXZ value, we easily find the central charge of the staggered vertex model:

$$c = 2. \quad (84)$$

Similarly to the XXZ model, the primary operators correspond to higher magnetization sectors (magnetic operators) and global shifts of the Bethe integers (electric operators). In the present situation, each set of roots $\{\lambda_j^0\}, \{\lambda_j^1\}$ can be excited independently, and we denote m^0, m^1 (resp. e^0, e^1) the magnetic (resp. electric) charges. The Wiener-Hopf technique²⁶ can be adapted¹³ to the \mathbb{Z}_2 BAE, and we obtain the conformal dimensions

$$h_{\underline{e}, \underline{m}} = \frac{1}{8} \left(\frac{e^+}{\sqrt{2g_1}} + m^+ \sqrt{2g_1} \right)^2 + \frac{1}{8} \left(\frac{e^-}{\sqrt{2g_2}} + m^- \sqrt{2g_2} \right)^2, \quad (85)$$

$$\bar{h}_{\underline{e}, \underline{m}} = \frac{1}{8} \left(\frac{e^+}{\sqrt{2g_1}} - m^+ \sqrt{2g_1} \right)^2 + \frac{1}{8} \left(\frac{e^-}{\sqrt{2g_2}} - m^- \sqrt{2g_2} \right)^2, \quad (86)$$

where $e^\pm := e^0 \pm e^1, m^\pm := m^0 \pm m^1$, and g_1, g_2 are encoded in the scattering kernels:

$$g_1 = \frac{1}{4} \left[1 - \frac{\widehat{K}^+(0)}{2\pi} \right], \quad g_2 = \frac{1}{4} \left[1 - \frac{\widehat{K}^-(0)}{2\pi} \right]. \quad (87)$$

The above spectrum corresponds exactly to two decoupled bosons as in (82). However, the electromagnetic charges obey the parity conditions

$$e^+ + e^- \equiv 0 [2], \quad m^+ + m^- \equiv 0 [2], \quad (88)$$

which introduce a coupling of the excitation sectors (or boundary conditions) for the two bosons. The vanishing of g_2 makes ϕ_2 a *non-compact* boson in the continuum limit, and each conformal exponent has a continuum of m^- magnetic states above it. The level density of this continuum is given by the finite-size scaling of g_2 . The latter can be calculated numerically for large but finite N , by solving the BAE in sectors with $m^- \neq 0$. One gets the following results

$$g_2(N) \propto \begin{cases} \left(\log \frac{N}{N_0} \right)^{-2} & \text{for } 0 \leq \gamma < \frac{\pi}{2}, \\ \left(\log \frac{N}{N_0} \right)^{-1} & \text{for } \gamma \rightarrow \frac{\pi}{2}, \end{cases} \quad (89)$$

where N_0 is a γ -dependent cut-off value. The numerical results for g_2 are shown in Fig. 4.

5.6. *Effective central charge and critical exponents*

In the presence of a twist φ , the conformal dimensions (85)–(86) are modified by the change $e^+ \rightarrow e^+ + \frac{2\varphi}{\pi}$. The ground state of the critical AF Potts model has a

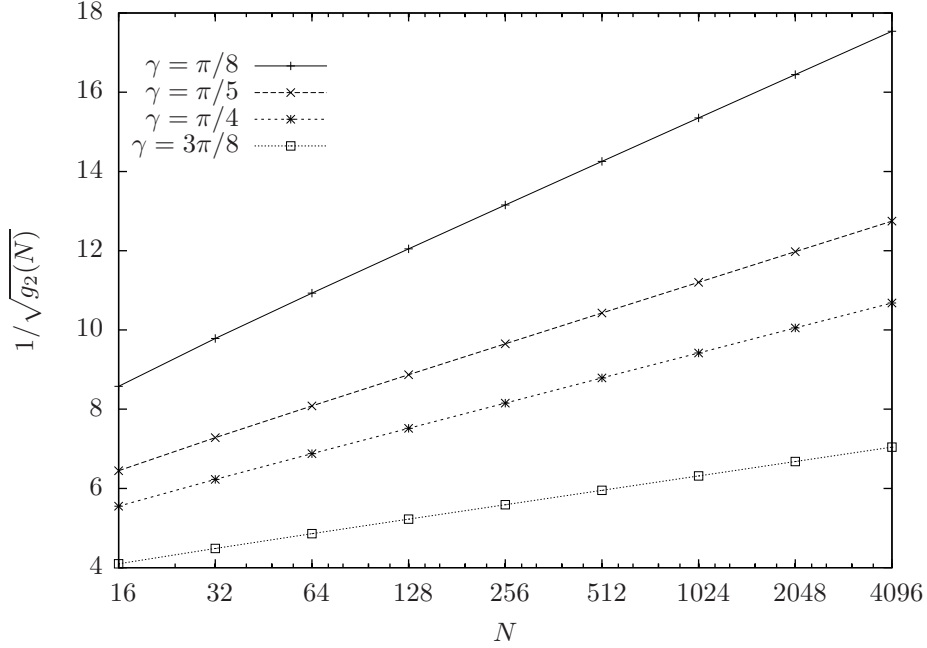


Fig. 4. Effective coupling constant of boson ϕ_2 for the AF critical line, for various values of γ . The data indicate that $g_2(N) \propto \left(\log \frac{N}{N_0}\right)^{-2}$.

twist $\varphi = \gamma$, and we denote $e_0 := \frac{\gamma}{\pi}$. The effective central charge is thus

$$c_{\text{eff}} = 2 - \frac{6e_0^2}{g_1} = 2 - \frac{6}{t}. \quad (90)$$

Similarly to Section 4.4, some critical exponents of the Potts model at the AF transition are obtained from various sectors of the \mathbb{Z}_2 vertex model.

- The ℓ -leg watermelon exponent has magnetic charge $m^+ = \frac{\ell}{2}$. The anti-symmetric magnetic charge does not contribute to the conformal dimension, since $g_2 = 0$. Hence:

$$X_\ell = \frac{g_1(\ell/2)^2}{2} - \frac{e_0^2}{2g_1} = \frac{\ell^2 - 4}{8t}. \quad (91)$$

- The ‘thermal sector’ with $m^+ = 0$ contains a state with twist $\varphi = \pi(e_0 - 1)$, and exponent:

$$X'_T = \frac{(e_0 - 1)^2 - e_0^2}{2g_1} = \frac{t - 2}{2}. \quad (92)$$

However, the first excited state in the Potts model has an exponent

$$X_T = \frac{2(t - 3)}{t - 2}, \quad (93)$$

which is not part of the electromagnetic spectrum (85)–(85). This exponent may be interpreted from parafermionic CFTs for integer t (see Section 7), and is valid for generic t .

- In the case of the magnetic exponent X_H , the expected value when setting the twist to $\varphi = \frac{\pi}{2}$ would be $X_H = \frac{(1/2)^2}{2g_1} - \frac{e_0^2}{2g_1} = \frac{t}{8} - \frac{1}{2t}$, but transfer-matrix calculations do not match this value. Rather, the magnetic exponent is

$$X_H = \frac{1}{4} - \frac{1}{2t}. \quad (94)$$

Again, this value is consistent with parafermionic CFT for integer t .

5.7. The limit $Q \rightarrow 0$

We consider the following limit:

$$\gamma = \frac{\pi}{2} + h, \quad u = hw, \quad w \text{ fixed}, h \rightarrow 0. \quad (95)$$

In this limit, the double-edge \check{R} -matrix for the loop model has the form:

$$-\frac{\check{R}}{h^2} \xrightarrow{h \rightarrow 0} (1-w) \mathbf{1} + w E + w(1-w) P := \check{R}_B(w), \quad (96)$$

where $\mathbf{1}$, E and P are defined by the diagrams in Fig. 5. The operators E_j and P_j generate a Brauer algebra with loop weight 0, defined by the relations

$$\begin{cases} P_j P_{j\pm 1} P_j = P_{j\pm 1} P_j P_{j\pm 1} \\ P_j^2 = \mathbf{1} \\ P_j P_k = P_k P_j \quad \text{for } |j-k| > 1 \end{cases} \quad \begin{cases} E_j E_{j\pm 1} E_j = E_j \\ E_j^2 = 0 \\ E_j E_k = E_k E_j \quad \text{for } |j-k| > 1 \end{cases} \quad (97)$$

$$\begin{cases} P_j E_j = E_j P_j = E_j \\ E_j P_{j\pm 1} P_j = E_j E_{j\pm 1} \\ P_{j\pm 1} P_j E_{j\pm 1} = E_j E_{j\pm 1} \end{cases} \quad (98)$$

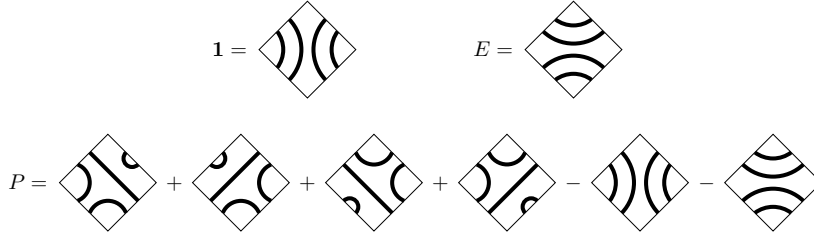
Moreover, in the above limit, the vertex model is equivalent to the supersymmetric $\text{OSP}(2|2)$ representation of the Brauer algebra. As a check, we can derive the $Q \rightarrow 0$ limit of the BAE, where $\lambda_j^a \rightarrow h\eta_j^a$:

$$\left(\frac{i + \eta_j^a}{i - \eta_j^a} \right)^N = (-1)^{r^a - 1} e^{2i\varphi} \prod_{\ell=1}^{r^{1-a}} \frac{2i + \eta_j^a - \eta_\ell^{1-a}}{2i - \eta_j^a + \eta_\ell^{1-a}}, \quad (99)$$

$$E = \sum_{a=0,1} \sum_{j=1}^{r^a} \frac{-4}{1 + (\eta_j^a)^2}, \quad (100)$$

which are indeed the $\text{OSP}(2|2)$ BAE.

Loop models based on the Brauer algebra are integrable, but do not admit a Coulomb-gas description because loop intersections are present. In fact, it was shown²⁸ that they correspond to a universality class distinct from the $\text{O}(n)$ model. For integer loop weight, they admit a Bethe-Ansatz solution related to the $\text{OSP}(n|2m)$ superalgebra²⁹.

Fig. 5. Generators of the Brauer model, built from the $TL_{2N}(n=0)$ algebra.

6. The anisotropic critical regime

In this Section, we describe the critical regime of the Potts model based on the \mathbb{Z}_2 staggered 6V model (like the AF critical line), in the range $0 < u < \gamma$ where the coupling constants x_1 and x_2 have opposite signs¹³ (see Table 1). We refer to this regime as the anisotropic critical regime. Since it is based on the same vertex model as the AF critical line, the Bethe-Ansatz analysis is very similar, and so we will simply emphasize the differences with the previous Section. The resulting CFT is also a combination of two decoupled bosons ϕ_1 and ϕ_2 , but in the present case, both bosons have a finite compactification radius. It is possible to write the toroidal partition sum as a generating series of conformal dimensions, and interpret ϕ_2 as a combination of two pairs of Majorana fermions.

6.1. Bethe Ansatz Equations

The Bethe roots are of two kinds:

$$\alpha_j^0 = \lambda_j^0, \quad \alpha_j^1 = \lambda_j^1 + i\pi, \quad (101)$$

and the BAE and energies read

$$\exp[iNk(\lambda_j^a)] = (-1)^{r^a-1} e^{2i\varphi} \prod_{b=0,1} \prod_{\ell=1}^{r^b} \exp[-i\Theta^{a-b}(\lambda_j^a - \lambda_\ell^b)], \quad (102)$$

$$E = \sum_{a=0,1} \sum_{j=1}^{r^a} \epsilon(\lambda_j^a) = \sum_{a=0,1} \sum_{j=1}^{r^a} \frac{-2 \sin^2 2\gamma}{\cosh 2\lambda_j^a - \cos 2\gamma}, \quad (103)$$

where:

$$k(\lambda) := -i \log \frac{\sinh(i\gamma - \lambda)}{\sinh(i\gamma + \lambda)}, \quad (104)$$

$$\Theta^0(\lambda) := -i \log \frac{\sinh(i\gamma + \frac{\lambda}{2})}{\sinh(i\gamma - \frac{\lambda}{2})}, \quad \Theta^{\pm 1}(\lambda) := -i \log \frac{\cosh(i\gamma + \frac{\lambda}{2})}{\cosh(i\gamma - \frac{\lambda}{2})}. \quad (105)$$

20 *Yacine Ikhlef*

States where $\{\lambda_j^0\} = \{\lambda_j^1\}$ are solutions of an XXZ model with $\mu = 2\gamma$. The ground state is a double Fermi sea with central charge $c = 2$. Quasi-particles are of two types 0, 1, with dispersion relation (36), and scattering kernels

$$\hat{\Phi}^0(\omega) = \frac{-2\pi \sinh(\pi - 3\gamma)\omega}{2 \cosh \gamma\omega \sinh(\pi - 2\gamma)\omega}, \quad \hat{\Phi}^{\pm 1}(\omega) = \frac{2\pi \sinh \gamma\omega}{2 \cosh \gamma\omega \sinh(\pi - 2\gamma)\omega}. \quad (106)$$

6.2. CFT spectrum and continuum partition function

The conformal spectrum has the same form (85)–(86) as for the AF critical point:

$$h_{\underline{e}, \underline{m}} = \frac{1}{8} \left(\frac{e^+}{\sqrt{2g_1}} + m^+ \sqrt{2g_1} \right)^2 + \frac{1}{8} \left(\frac{e^-}{\sqrt{2g_2}} + m^- \sqrt{2g_2} \right)^2, \quad (107)$$

$$\bar{h}_{\underline{e}, \underline{m}} = \frac{1}{8} \left(\frac{e^+}{\sqrt{2g_1}} - m^+ \sqrt{2g_1} \right)^2 + \frac{1}{8} \left(\frac{e^-}{\sqrt{2g_2}} - m^- \sqrt{2g_2} \right)^2, \quad (108)$$

now with finite coupling constants

$$g_1 = \frac{\pi - 2\gamma}{2\pi}, \quad g_2 = \frac{1}{2}. \quad (109)$$

The parity conditions also hold:

$$e^+ + e^- \equiv 0 \pmod{2}, \quad m^+ + m^- \equiv 0 \pmod{2}. \quad (110)$$

In this context, the toroidal partition function can be written as a generating function for the conformal weights, and it reflects the coupling of the BC:

$$Z_{\text{stag. 6V}} = \frac{1}{|\eta(q)|^4} \sum_{\substack{e^+ + e^- \equiv 0 \pmod{2} \\ m^+ + m^- \equiv 0 \pmod{2}}} q^{h_{\underline{e}, \underline{m}}} \bar{q}^{\bar{h}_{\underline{e}, \underline{m}}}. \quad (111)$$

The factors associated to charges e^-, m^- are bosonic partition sums with coupling constant $g_2 = \frac{1}{2}$, which can be written as products of *two* Ising partition sums with various BC. We introduce the Ising partition sum $\mathcal{Z}_{r, r'}$, with BC on the Ising spins $\sigma \rightarrow (-1)^r \sigma, \sigma \rightarrow (-1)^{r'} \sigma$, and the bosonic partition sum $Z_{m, m'}(g)$, with BC $\phi \rightarrow \phi + 2\pi m, \phi \rightarrow \phi + 2\pi m'$. The partition function reads¹³

$$Z_{\text{stag. 6V}} = \frac{1}{2} \sum_{\substack{m \equiv r_1 + r_2 \pmod{2} \\ m' \equiv r'_1 + r'_2 \pmod{2}}} (-1)^{r_1 r'_2 + r'_1 r_2} \mathcal{Z}_{r_1, r'_1} \mathcal{Z}_{r_2, r'_2} Z_{m, m'}(g_1). \quad (112)$$

In this form, the \mathbb{Z}_2 model appears as two Ising models and one compact boson, decoupled in the bulk and coupled through their BC.

6.3. Effective central charge and critical exponents

In the presence of a twist φ , the conformal dimensions (107)–(107) are modified by the change $e^+ \rightarrow e^+ + \frac{2\varphi}{\pi}$. Like for the AF line, we denote $e_0 := \frac{\gamma}{\pi}$, and the ground state has a twist $\varphi = \pi e_0$. The effective central charge is thus

$$c_{\text{eff}} = 2 - \frac{6e_0^2}{g_1} = 2 - \frac{12}{t(t-2)}. \quad (113)$$

- The ℓ -leg watermelon exponent has magnetic charge $m^+ = \frac{\ell}{2}$. Because of the parity condition (110), the lowest possible value for the antisymmetric magnetic charge m^- is 0 for even m^+ and 1 for odd m^+ . As a consequence, the watermelon exponents are

$$X_\ell = \begin{cases} \frac{g_1(\ell/2)^2}{2} - \frac{e_0^2}{2g_1} & \text{if } \ell \equiv 0 \pmod{4} \\ \frac{g_1(\ell/2)^2}{2} + \frac{1}{4} - \frac{e_0^2}{2g_1} & \text{if } \ell \equiv 2 \pmod{4}. \end{cases} \quad (114)$$

- In the thermal sector with twist $\varphi = e_0$, the energy exponent corresponds to charges $e^+ = 2e_0 - 2$, $e^- = 0$, which gives the constant value

$$X_T = \frac{(e_0 - 1)^2 - e_0^2}{2g_1} = 1. \quad (115)$$

This is equivalent to the energy excitation in one of the Ising models.

- The magnetic exponent X_H is given by the twist $\varphi = \frac{\pi}{2}$. It turns out that the lowest exponent in this twist sector has electric charges $e^+ = \frac{2\varphi}{\pi} - 1$, $e^- = 1$. The exponent is thus

$$X_H = \frac{1}{4} - \frac{e_0^2}{2g_1}. \quad (116)$$

7. Conclusion

The Q -state Potts model is a simple lattice model, in which the ferromagnetic critical point provides a basic realization of minimal CFTs. The antiferromagnetic part of its phase diagram has been less studied than the ferromagnetic one, but it contains three critical regimes of physical interest for Statistical Mechanics and Condensed Matter Theory. In this review, we have shown that, through an equivalence to loop and vertex models, these critical points can be solved by Bethe Ansatz. This approach is powerful enough to discover the CFT spectrum, the S -matrix description of quasi-excitations, and also the critical exponents in the original statistical model.

Most of the material exposed in this review is valid for generic values of Q . When Q is a Beraha number ($Q = 4 \cos^2 \frac{\pi}{t}$, with t integer), the Potts model can be mapped to an RSOS height model (see Section 2.3). Although the partition functions of the two models are identical (even at the lattice level), the excitation spectra can be very different. The essential mechanism at play is that some excited states of the vertex model have a vanishing contribution to the RSOS partition function. In

the CFT language, the elimination of these states amounts to *null-state equations*, which are the basis for the determination of minimal series of CFTs. RSOS models with homogeneous Boltzmann weights (corresponding to the self-dual Potts model) were shown to have four different physical phases I,II,III,IV, with critical transitions separating phases III-IV and I-II. These two transitions are lattice realizations of the Minimal and \mathbb{Z}_k -parafermionic (for $k = t - 2$) CFTs, respectively³⁰.

Back to the Potts model with Beraha values, this tells us that the RSOS version of the ferromagnetic critical point relates to a Minimal CFT, whereas that of the BK phase relates to the \mathbb{Z}_k -parafermionic CFT. The question of the RSOS version for the AF critical line is more difficult, but it has been found recently¹¹ that this is also described by the \mathbb{Z}_k -parafermionic CFT. This relation is supported by the study of critical exponents and of the algebra of chiral currents.

Although the critical phases of the antiferromagnetic Potts model are now identified and well studied, there remain interesting open questions to the mathematical physicist.

From the point of view of integrable models, the understanding of the \mathbb{Z}_2 model would be more complete if one could extend the relation to braiding algebras (see Section 5.7). Also, an analytic derivation of the effective coupling constant for the non-compact boson should be possible. Moreover, one can generalize the \mathbb{Z}_2 construction to a \mathbb{Z}_p six-vertex model, where the \mathbb{Z}_p symmetry will be reflected in the whole Bethe-Ansatz structure. This opens a new series of models, similarly to what appears in the fusion procedure.

Finally, the Potts model is a good framework to study the physics of cluster or spin interfaces in lattice models. Current studies focus on the links between boundary CFT, Schramm-Löwner Evolution (SLE) and free massless field theories. In the case of the antiferromagnetic Potts model, the Fortuin-Kasteleyn cluster boundaries are well described by the ℓ -leg watermelon exponents, all related to the first boson ϕ_1 , but the geometric expression of the second boson ϕ_2 is lacking. This additional degree of freedom may lead to an extended version of the SLE process, as was introduced recently^{31,32}.

Acknowledgements

The author thanks J. Jacobsen and H. Saleur for their help with the preparation of this paper.

References

1. R. B. Potts, *Proc. Camb. Phil. Soc.* **48** (1952) 106.
2. R. J. Baxter, *Exactly Solved Models in Statistical Mechanics* (Academic Press, London, 1982).
3. B. Nienhuis, in *Phase Transitions and Critical Phenomena* vol. **11**, ed. C. Domb and J.L. Lebowitz (Academic Press, London, 1987).
4. Ph. Di Francesco, H. Saleur and J.-B. Zuber, *J. Stat. Phys.* **49** (1987) 57.

5. Ph. Di Francesco, P. Mathieu and D. Sénéchal, *Conformal Field Theory* (Springer, New York, 1997).
6. R. J. Baxter, *Proc. R. Soc. Lond.* **383** (1982) 43.
7. H. Saleur, *Commun. Math. Phys.* **132** (1990) 657.
8. H. Saleur, *Nucl. Phys.* **B360** (1991) 219.
9. A. B. Zamolodchikov and V. A. Fateev, *Zh. Eksp. Theor. Fiz.* **89** (1985) 380.
10. H. Au-Yang and J. H. H. Perk, *Int. J. Mod. Phys.* **A7**, Suppl. **1B** (1992) 1025.
11. J. L. Jacobsen and H. Saleur, *Nucl. Phys.* **B743** (2006) 207.
12. Y. Ikhlef, J. L. Jacobsen and H. Saleur, *Nucl. Phys.* **B789** (2008) 483.
13. Y. Ikhlef, J. L. Jacobsen and H. Saleur, *J. Phys.* **A43** (2010) 225201.
14. C. M. Fortuin, P. W. Kasteleyn, *Physica* **57** (1972) 536.
15. H. N. V. Temperley and E. H. Lieb, *Proc. R. Soc. Lond.* **A322** (1971) 251.
16. R. Kenyon, *J. Math. Phys.* **41** (2000) 1338.
17. S. Caracciolo *et al.*, *Phys. Rev. Lett.* **93** (2004) 080601.
18. J. L. Jacobsen and H. Saleur, *Nucl. Phys.* **B716** (2005) 439.
19. V. Pasquier and H. Saleur, *Nucl. Phys.* **B330** (1990) 523.
20. Y. Ikhlef, J. L. Jacobsen and H. Saleur, *J. Phys.* **A42** (2009) 292002.
21. C. K. Majumdar and D. K. Ghosh, *J. Math. Phys.* **10** (1969) 1388,1399.
22. S. R. White and I. Affleck, *Phys. Rev.* **B54** (1996) 9862.
23. M. T. Batchelor and C. M. Yung, *Int. J. Mod. Phys.* **B8** (1994) 3645.
24. G. E. Andrews, R. J. Baxter and P. J. Forrester, *J. Stat. Phys.* **35** (1984) 193.
25. V. Pasquier *Nucl. Phys.* **B285** (1987) 162.
26. C. N. Yang and C. P. Yang, *Phys. Rev.* **150** (1966) 321;
Phys. Rev. **150** (1966) 327.
27. V. E. Korepin, N. M. Bogoliubov and A. G. Izergin *Quantum Inverse Scattering Method and Correlation Functions* (Cambridge University Press, 1997).
28. J. L. Jacobsen, N. Read and H. Saleur, *Phys. Rev. Lett.* **90** (2003) 090601.
29. M. J. Martins, B. Nienhuis, R. Rietman, *Phys. Rev. Lett.* **81** (1998) 504.
30. D. A. Huse, *Phys. Rev.* **B 30** (1984) 3908.
31. E. Bettelheim, I. A. Gruzberg, A. W. W. Ludwig and P. Wiegmann, *Phys. Rev. Lett.* **95** (2005) 170602.
32. R. Santachiara, *Nucl. Phys.* **B 793** (2008) 396.